Zhang, Shiying; Meinhard, Halvar; Collins, Steven; Lourencon, Tainise V.; Rautkari, Lauri

Effect of ionic liquid [emim][OAc] on the set recovery behavior of densified wood

Published in:
Cellulose

DOI:
10.1007/s10570-024-06043-z

Published: 01/09/2024

Document Version
Publisher's PDF, also known as Version of record

Cellulose (2024) 31:8267–8278
https://doi.org/10.1007/s10570-024-06043-z

ORIGINAL RESEARCH

Effect of ionic liquid [emim][OAc] on the set recovery behavior of densified wood

Shiying Zhang · Halvar Meinhard · Steven Collins · Tainise V. Lourencon · Lauri Rautkari

Received: 7 March 2024 / Accepted: 30 June 2024 / Published online: 14 August 2024

Abstract Wood modification techniques, like densification, can improve the mechanical performance of low-density and undervalued wood species, rendering them suitable for high-value engineering applications. Nevertheless, densified wood (DW) commonly manifests a set recovery (SR) phenomenon when exposed to water, negating the enhancements achieved through densification. Our method addresses the SR issue and the non-recyclability associated with conventionally produced DW using chemical techniques in wood densification. To mitigate SR in DW, an ionic liquid (IL) 1-ethyl-3-methylimidazolium acetate was impregnated as a cellulose plasticizing agent prior to wood densification. This method facilitated permanent deformation within the cellulose network, resulting in negligible SR. Moreover, the DW treated with IL (DW_1w) demonstrated an increase in both modulus of rupture and modulus of elasticity after water washing and subsequent redrying, in comparison to the untreated control (UC). Notably, spectroscopic (FTIR) analyses indicated that the chemical structure of DW_1w remained akin to that of UC. Additionally, the IL leached out during the DW-water washing step can be recovered. This research contributes to advancing sustainable alternatives to less ecologically friendly (chemical) pretreatment methods to reduce SR related issues in DW.

Keywords Wood densification · Ionic liquid · Set recovery · Bending strength · Recyclability

Introduction

The current trend in material processing industries is to adopt the principles of green chemistry, decarbonization, and sustainability (Liu et al. 2021; Rissman et al. 2020). Wood, being a renewable forestry resource, holds large potential to foster sustainability across various industries, notably those involving construction and building elements (Dong et al. 2022). By capitalizing on its intricate and hierarchical structure, densifying sawn timber may contribute to a substantial enhancement in mechanical properties, such as modulus of rupture (MOR), modulus of elasticity (MOE), and hardness, creating new market opportunities for utilizing low-density wood species as raw material for high-value engineering applications (Cabral et al. 2022; Luan et al. 2022; Neyses et al. 2020; Song et al. 2018). One of the major obstacles hindering its commercialization is the set recovery (SR) of densified wood (DW) upon exposure to

Supplementary Information The online version contains supplementary material available at https://doi.org/10.1007/s10570-024-06043-z.

S. Zhang · H. Meinhard · S. Collins · T. V. Lourencon · L. Rautkari (✉)
Department of Bioproducts and Biosystems, School of Chemical Engineering, Aalto University, 02150 Espoo, Finland
e-mail: lauri.rautkari@aalto.fi

water (Neyses et al. 2020). This phenomenon refers to the compressed wood cells reverting essentially to their original shape under the influence of moisture, thereby considerably depreciating the improvements in the material properties achieved through the densification process (Neyses et al. 2020). Current techniques employed to reduce SR in wood densification involve heat stabilization (thermal modification), such as thermo-mechanical or thermo-hydro-mechanical densification of timber, or the impregnation of wood with chemicals like phenol–formaldehyde or melamine–formaldehyde (Cabral et al. 2022). However, the heat stabilization method induces a significant reduction in wood mechanical strength. Moreover, impregnating wood with resins raises environmental concerns and poses challenges for wood recycling and cascading (Cabral et al. 2022; Neyses et al. 2020). According to the proposed SR mechanism, it is hypothesized that if plastic deformation of crystalline cellulose can be achieved prior to or during the densification process, the SR can be reduced (Neyses et al. 2021). This hypothesis presents an intriguing opportunity to develop efficient and environmentally friendly techniques for plasticizing crystalline cellulose without compromising its mechanical strength. Such advancements hold the potential to advance the field of wood densification towards more sustainable processes and utilization.

The discovery of Ionic liquids (ILs) capable of dissolving cellulose has prompted extensive research over the past two decades, exploring ILs as a green agent for the pretreatment, dissolution, and conversion of lignocellulose materials (Qasim et al. 2021). Additionally, the application of ILs in wood modification has demonstrated enhanced resistance to fire and resistance against fungi and termite decay in wood, as evidenced by preceding studies (Miyafuji and Fujiwara 2013; Abu-Eishah 2015; Croitoru and Roata 2020; Neyses et al. 2020; Miyafuji and Minamoto 2022;). Specifically, imidazolium cationic ILs containing an acetate anion, such as 1-ethyl-3-methylimidazolium acetate ([emim][OAc]), has demonstrated a significant cellulose dissolution capacity (Sun et al. 2009; Zhang et al. 2024). Besides that, [emim][OAc] can completely solubilize softwood species (Khakalo et al. 2020) and is considered as a green solvent in regard to non-hazardous chemical compound emitting during utilization, handling, and transportation. (Abushammala and Mao 2020). Halder and coauthors indicated that the recycling of [emim][OAc] used in lignocellulose pretreatment, can achieve a recovery rate exceeding 85%, with no observed chemical structural alternations (Halder et al. 2020). This suggests that ILs offer potential advantages in terms of enhancing process efficiency and bolstering sustainability in terms of recycling, recovery, and reusability.

A limited number of studies related to the utilization of ILs in wood densification have been reported, such as Neyses et al. (2020) conducting studies on wood surface densification subjected to an IL [Bmim][Cl] treatment at a high temperature (270 °C), revealing reduction in SR to approximately 10%. Additionally, Khakalo et al. (2019, 2020) utilized [emim][OAc] to partially dissolve the fiber surface of delignified veneers, integrating it with densification to fabricate structural materials and all-wood composites. However, the IL treatment in bulk wood densification is not yet thoroughly explored and the complete reduction of SR in DW is not yet addressed.

In this work, we introduce a feasible and recyclable manufacturing process to produce DW endowed with high dimensional stability (near to zero SR) against moisture to address the aforementioned challenges related to wood densification. This accomplishment is realized through the integration of an IL ([emim][OAc]) treatment to soften wood polymers at 150 °C, followed by a post-treatment involving water washing of DW and subsequent redrying. In addition to investigating the SR behavior of the DW, we conducted a comprehensive analysis of its flexural strength, thermal stability, and chemical structure. These in-depth assessments serve to substantiate the potential applications of the produced material, including but not limited to use in structural applications, wooden floors, and wall panels. The proposed manufacturing method not only addresses challenges related to wood densification but also provides preliminary findings aligned with sustainability goals through its recyclable nature.

Materials and methods

The entire procedure of the DW production is schematically illustrated in Fig. 1. The initial step involves fabricating the DW by impregnating clear wood with [emim][OAc] diluted in ethanol, serving as a cellulose plasticizing agent. Following ethanol evaporation, the

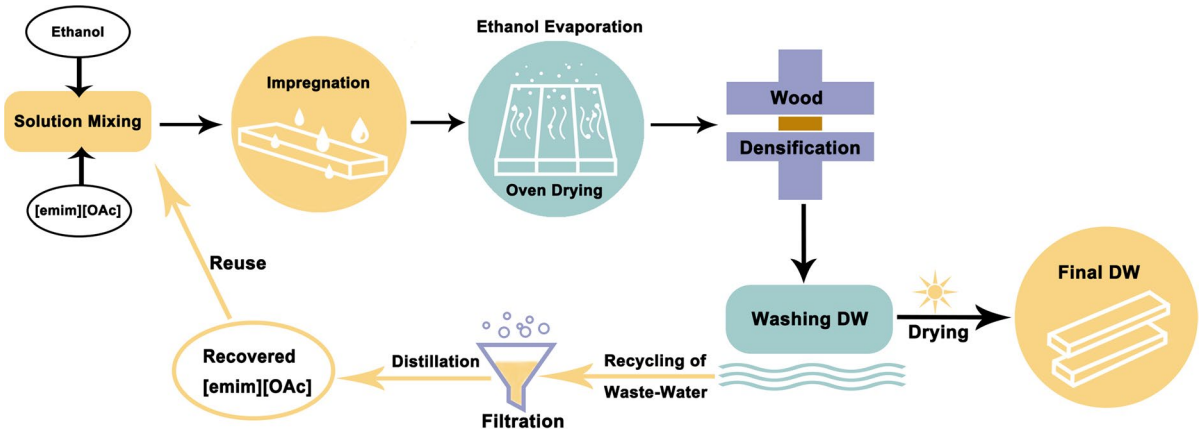

Fig. 1 Schematic illustration of the circular production process for IL-pretreated densified wood

impregnated wood is subjected to compression by a hydraulic press. Subsequently, the DW undergoes a washing procedure with deionized water to reclaim the [emim][OAc]. The resulting washed DW is then subjected to drying and conditioning for subsequent utilization. Additionally, the recovered [emim][OAc] is reused in further wood treatment.

Wood impregnation and densification

Clear wood (Scots pine/*Pinus sylvestris* L., south-eastern Finland) was cut to blocks showing parallel annual rings on the longitudinal cross-section. IL [emim][OAc] (Proionic, Austria) was diluted with ethanol (ETAX Aa, Anora, Finland) to create a 35 wt% IL-ethanol solution for wood impregnation. It is important to note that employing ethanol as an IL carrier for wood impregnation facilitates rapid evaporation/drying at a low temperature (50 °C) without inducing wood degradation. Wood impregnation with IL-ethanol solution (IW_IL) was performed in a vacuum oven (Thermo Scientific, VT 6025, Fisher Scientific Oy, Finland) at 200 Pa and 20 °C until wood specimens settled down to the bottom of the solution. Subsequently, IW_IL samples were subjected to drying in an oven at 50 °C overnight (16 h) to evaporate the ethanol.

The wood densification process was carried out using a hydraulic press (Vakomet KRO-260, Lakeuden Hydro Oy, Finland). The wood blocks were radially compressed from their original dry thickness (10 mm at 0% MC) employing a 5 mm thick stainless-steel plate as the compression stop. The target thickness of 5 mm was reached by applying a quick incremental displacement of 9.9 mm/s (in accordance with EN 693) and then holding at the target thickness for a duration of 0.5 h, for IL treated specimens, and 1 h otherwise. Subsequently, IL treated DW samples were subjected to washing with a deionized water bath (20 °C). The water bath was exchanged in 3 h-intervals until no color change of the washing water was observable, indicating complete removal of the IL from the specimens, then followed by redrying to stabilize the structure of DW. It is noteworthy that the temperature employed (150 °C) is intentionally below the conventional wood heat-treatment temperature range (180–250 °C) (Candelier et al. 2016). This decision was made to exclude the potential effect of heat-induced stabilization on wood structure, providing a clear understanding of IL impact on wood polymers at a milder temperature. To ensure the complete elimination of IL from treated wood, FTIR was performed.

The corresponding DW samples will hereafter be denoted as DW_n, where the n signifies the compression duration of the wood. Therefore, the specimens are sorted into sample groups, including untreated control wood (UC), densified wood without IL impregnation (UCDW), UCDW following immersion in water and subsequent oven drying (UCDW_w), densified wood with IL impregnation (DW_n), and DW_n after washing with deionized water (DW_nw). Detailed information of sample groups subjected to

set-recovery analysis and mechanical tests is provided in Table S1.

Set recovery and mechanical properties

The SR behavior of DW was investigated by immersing 4 replicates from each sample group (Table S1) in deionized water for two cycles of wet-dry. The 1st cycle involving 24 h submersion in water, followed by overnight oven drying at 105 °C. The 2nd cycle involving 72 h submersion in water, followed by subsequent oven drying at 105 °C overnight. A digital caliper was employed to measure the thickness change of the specimens. The set recovery was determined according to Eq. 1 (Rautkari et al. 2010):

$$SR = \frac{T_r - T_d}{T_o - T_d} * 100 \quad (1)$$

where T_r is the thickness of DW at the end of wet-dry cycles. T_d is the thickness of UCDW after compression, and for IL treated DW, the T_d is the thickness of DW after water washing and subsequent redrying overnight at 105 °C. T_o is the thickness of wood samples in a dry state before the densification process.

Mechanical properties of DW were evaluated through 3-point bending tests using a universal material testing device (Zwick 1475, Zwick Roell AG, Germany) at a continuous loading rate of 5 mm/min. Prior to testing, the samples were conditioned at a relative humidity (RH) of 65% and 20 °C until achieving equilibrium moisture content. Ten replicates of each sample group were analyzed, and the bending load was radially applied to the specimens. The modulus of rupture (MOR) was calculated according to Eq. 2 (SFS-EN 310 2001):

$$MOR = \frac{3F_{max}l_1}{2bt^2} \times 100 \quad (2)$$

where F_{max} is the maximum load (N) at which the sample ruptures. l_1 denotes the distance (mm) between the respective center of the roller-bearing supports, which is 20 times the radial thickness (t) of the specimens (however, the l_1 for the UC and UCDW_w is about 10 times the (t). The parameter b represents the width (mm) of the test pieces in the tangential direction. The modulus of elasticity (MOE) was determined following Eq. 3 (SFS-EN 310 2001):

$$MOE = \frac{l_1^3\left(F_2 - F_1\right)}{4bt^3\left(a_2 - a_1\right)} \quad (3)$$

where the quantity $F_2 - F_1$ represents the load increment on the linear portion of the load–deflection curve in Newtons. F_1 corresponds to 10% of the maximum load (F_{max}), while F_2 was 40% of F_{max}. The same principle is applied to the deflection increment ($a_2 - a_1$) at the mid-length of the test samples.

Morphology and molecular structural features

The dynamic SR behavior of the test samples was monitored using transmitted light microscopy (Olympus, BX53M, Japan). This monitoring involved immersing a piece of DW (40 µm thickness) in water on a designed glass slide for 24 h, with images captured at different time intervals. Cross-section morphology of DW was investigated by SEM (Zeiss, Sigma VP, Germany). The molecular structure of samples was characterized by FTIR-ATR spectroscopy (PerkinElmer, UK). Each measurement was conducted with 16 scans at 4 cm^{-1} resolution, and the spectra were corrected by a scan without a sample loaded, yielding the background spectrum of ambient air.

Thermostability of wood samples

The changes in the thermostability of DW were determined using thermogravimetric analysis (Thermo-Gravimetric Analyzer Q500, TA Instruments, USA) in a nitrogen atmosphere. The DW specimens were cut into granules before loading 10 mg onto the pan, and the samples were subsequently heated from 30 to 600 °C with a 10 °C/min heating ramp. The changes in sample mass as a function of temperature were recorded.

Results and discussion

Set recovery and mechanical properties of densified wood blocks

Table 1 provides a summary of the SR and mechanical property results for the investigated groups. Evidently, the densified control sample (UCDW), when

Table 1 Mean values of set recovery, density, modulus of rupture and modulus of elasticity with the thickness (T_r) in bending test of investigated samples, with standard deviation in parenthesis

Sample	SR (%)		Density (kg/m^3)	MOR (N/mm^2)	MOE (kN/mm^2)	T_r(mm)
	1st cycle	2nd cycle	RH_0%	RH_65%	RH_65%	RH_65%
UC	-	-	484(31.4)	103.9(16.4)	8.4(1.3)	10.2(0.1)
UCDW	-	-	886(57.5)	220.7(41.8)	17.3(3.4)	5.1(0.1)
UCDW_w	79.1(3.6)	85.6(3.4)	508(41.5)	65.7(7.9)	5.0(0.6)	9.4(0.1)
DW_0.5w	2.6(1.9)	0.2(1.5)	863(47.9)	-	-	-
DW_1w	0.8(2.3)	0.2(0.6)	899(21.2)	163.7(11.1)	17.1(1.0)	5.1(0.3)

subjected to water exposure (UCDW_w), demonstrated a mean SR of approximately 79.1%, implying a significant structural deformation upon contact with water and subsequent redrying (Fig. 2). Notably, the SR became more pronounced after the 2nd cycle of wet-dry (Table 1). This increased SR can be attributed to a prolonged submersion time (72 h) in water, allowing cellulose to thoroughly release the internal stress resulting from the compression process (Neyses et al. 2020). Although UCDW had the highest values for both MOR and MOE among all tested sample groups, being roughly twice as high as those of the UC (Table 1), the SR of UCDW upon water contact (UCDW_w) was also the most pronounced (Fig. 2). This is a critical consideration because the pronounced SR-induced shape deformation could potentially lead to structural failure of the wood during its service life, especially in application where contact with moisture is unavoidable, such as in flooring and outdoor applications. In addition, the flexural strength of UCDW_w (Table 1) evidently indicates a reduction in mechanical strength of UCDW after exposure to water and reconditioning, with both MOR and MOE even deteriorating beyond the level observed in the UC. This underlines the importance of addressing the SR phenomenon in DW to ensure the structural durability and performance of the material in practical applications.

In this regard, the introduction of IL as a cellulose plasticizing agent in wood densification demonstrated high efficacy in reducing SR. The samples impregnated with IL and subjected to compression for a duration of 0.5 h (DW_0.5w) and 1 h (DW_1w) exhibited negligible SR (Table 1), highlighting the effectiveness of an IL in mitigating the undesired deformation of DW associated with internal stress and water exposure. The sustained negligible SR of the IL treated samples, extending to repeated wet-dry cycles, implies that plastic deformation of crystalline cellulose occurred during the densification process due to the reaction with IL (Neyses et al. 2020, 2021).

Although both DW_0.5w and DW_1w show negligible SR, DW_1w exhibits a better structural stability in terms of SR. This enhanced performance of DW_1w may be attributed to the extended interaction of IL with wood polymers during the compression process. Notably, it has been observed that both the duration of the reaction and the heating temperature significantly impact the swelling, depolymerization or liquefaction, and fusion of wood polymers in IL (Miyafuji et al. 2009; Orelma et al. 2021). This relationship is further elucidated in Fig. S1, where a longer compression duration results in a slightly higher compression ratio, both before and after washing with water, followed by subsequent redrying. Specifically, DW_1w has a comparable compression ratio (45.5%) to that of UCDW (44.9%) after the leaching of IL during the water-washing process. This phenomenon indicates a gradual softening/dissolution of cellulose in wood through the IL treatment process, consistent with the findings of Orelma et al. (2021) and Miyafuji et al. (2009). Furthermore, the plasticization of cellulose can be attributed to the partial dissolution of cellulose during the impregnation and compression procedures. This phenomenon is evidenced in the

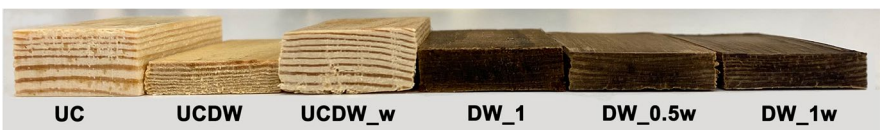

Fig. 2 The appearance of wood samples in dry state after each treatment

X-ray diffraction pattern of wood specimens (Figure S2), where the intensity of the diffraction peak around 2θ = 15° (1–10) in untreated cellulose (UC) is diminished in DW_1, indicating the plasticizing (softening) of cellulose. Conversely, the peak is restored in DW_1w (2θ = 14.8°), signifying that during the washing step, the recrystallization of dissolved cellulose chains in the anti-solvent occurs, creating strong intra- and inter-molecular interactions (Ling et al. 2017). Moreover, the 1-h treatment with [emim][OAc] induced a shift in peaks from 2θ = 22.3° (200) and 15° (1–10) of UC to 22° and 14.8° (extending to 12.5°) in DW_1w (Ling et al. 2017). These results further support the notion that IL-plasticization of cellulose occurs during compression (DW_1) and recrystallization in the washing stage (DW_1w). Consequently, it can be inferred that 1 h of IL treatment at 150 °C is sufficient to maintain the constant thickness of the specimens.

To further substantiate our hypothesis regarding the reusability of the recovered IL from the washing process (See the Ionic Liquid Recovery section in SI), the SR of the recovered IL-treated samples was analyzed and is illustrated in Fig. S3a. Evidently, in line with the findings from the initial IL-treated compressed wood (DW), a 1 h compression duration led to lower SR (0.3%) in DW when compared to a 0.5 h compression (3.6% SR). Additionally, the average SR value (Fig. S3a) of the recovered IL-treated DW indicates that the recovered IL has a comparable efficiency for cellulose plasticization. Especially noteworthy is the high similarity in the chemical structure of the recovered [emim][OAc] to that of the initial [emim][OAc], as illustrated in Fig. S3b. This result indicates that there might be no alteration in the chemical structure of the recovered [emim][OAc]. Importantly, this observation aligns with the finding reported by Halder et al. (2019, 2020), emphasizing the chemical stability of the [emim][OAc] during the recovery process.

It is crucial to note that the precise determination of the purity and percentage of the recovered [emim][OAc] was not undertaken, as our primary objective was to assess the reusability potential of the IL. Therefore, a precise characterization of the recovered IL's chemical composition and the IL recovery rate will be undertaken in our future studies. The current preliminary results in this study strongly indicate the potential reusability of [emim][OAc] as a plasticizing agent to reduce or even eliminate the SR in the wood densification process.

While achieving negligible SR in IL-treated DW resulted in a reduction in the modulus of rupture (MOR) compared to that of UCDW, the MOE of DW_1w remained comparable to the MOE of UCDW. Moreover, the respective MOR (163.7 N/mm^2) and MOE (18.0 kN/mm^2) of DW_1w demonstrate 1.6-fold increase in MOR and a twofold increase in MOE compared to those of UC (Table 1). These enhanced flexural strength and stiffness in wood specimens can be attributed to the densification treatment, as reported in a previous study (Xu et al. 2020). However, the apparent reduction in MOR for DW_1w compared to UCDW might be associated with polymer degradation during the heating, washing and redrying processes. This association arises from the fact that the IL utilized in the densification treatment can depolymerize wood polymers under heating conditions, and the subsequent water washing step can induce a reforming of the cellulose chain (Khakalo et al. 2019; Miyafuji et al. 2009; Orelma et al. 2021). Despite this MOR reduction, it is crucial to note the corresponding increase in MOE and the substantial mitigation of SR in DW_1w. These outcomes highlight the potential of using ILs in enhancing the overall mechanical performance and stability of DW.

Morphology and dynamic deformation of DW in water

The cross-section morphology of wood samples before and after densification are illustrated in Fig. 3a-d. Upon examination of Fig. 3a-b, it is evident that the morphology of IW_IL shows no discernible difference from that of the UC. This indicates that the employed IL impregnation with subsequent evaporation of ethanol method has no negative impact on the microstructure of the wood samples. (Any intense light reflection observed in the SEM images is likely attributed to the uneven surface of the samples, possibly arising from the sample preparation process.) The SEM micrographs of the densified samples (Fig. 3c-d) visually illustrate that densification mainly occurred within the earlywood region, with negligible deformation observed in the latewood region (a detailed feature in Fig. S4b and Fig. S4e).

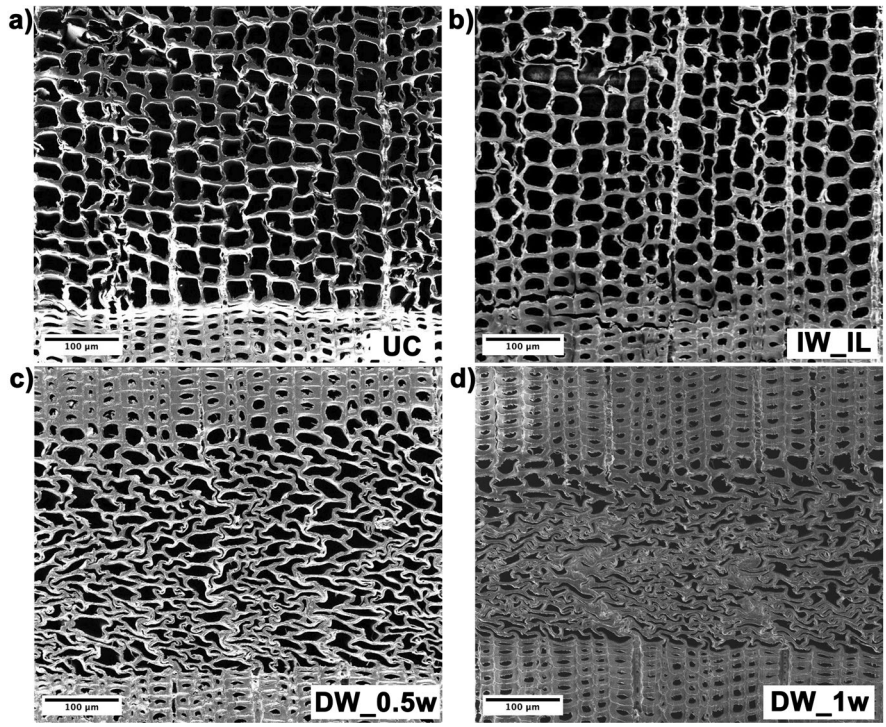

Fig. 3 SEM images of wood specimens before and after densification: **a** the cross-section morphology of the untreated control specimen; **b** the morphology of IL-impregnated wood prior to densification; **c** and **d** show the deformation patterns of the DW samples after water-washing and subsequent redrying

This phenomenon could be attributed to the thicker cell walls present in the latewood and the fact that the samples were compressed to only 42 to 46% (Fig. S1) of their initial thickness. Moreover, in softwood, the latewood cell walls provide mechanical strength and are characterized by their denser structure, while the earlywood, with larger lumina, primarily facilitates water transportation (Chen et al. 2020). Consequently, the cell walls of earlywood are more prone to deformation than those of the latewood.

Upon comparing the micro-morphology of DW_1w (Fig. 3c) to that of DW_0.5w (Fig. 3d). It is obvious that DW_1w demonstrates a denser structure in the compressed earlywood region. This observation aligns with the previously mentioned results, indicating that a 1 h compression duration resulted in slightly higher density and almost zero SR (Table 1).

Importantly, the absence of pronounced cracks or fractures within the compressed earlywood (Fig. 3c-d) and the observed interlocked or fused cell walls (Fig. 4b-c) suggest plastic deformation, likely induced by the softening effect of the IL (Nakaya et al. 2018). Noteworthy is the magnified detail of the selected section (Fig. 4c), which highlights the IL-induced merging of adjacent cell walls. This is particularly notable when compared to the micro-morphology of the densified specimen without IL treatment (Fig. S4b-c), where an hour of heat compression treatment (150 °C) did not mitigate the water-induced SR. Furthermore, the pronounced deformation (SR) of UCDW_w even induced minor cell wall cracks (Fig. S4c). This observation further validates our hypothesis that 1 h compression with IL ([emim][OAc]) treatment at 150 °C is adequate to maintain the constant thickness of the DW.

The dynamic changes in the morphology (Fig. 4d-e) of DW specimens upon exposure to water at different exposure times offer a deeper view of the set-recovery behavior between control specimens and wood subjected to IL treatment. Evidently, the compressed cell wall and lumen of UCDW (Fig. 4d) promptly revert towards their original configuration, manifesting marginal cell wall deformation. Within 30 min, the cell wall structure stabilizes, displaying no obvious subsequent alterations. Conversely, discernible alternations are absent within the distorted cell wall and lumen of DW_1w (Fig. 4e), barring a slight cell wall swelling attributed to water absorption. This phenomenon signifies the effective suppression of water-induced SR in DW facilitated by IL treatment.

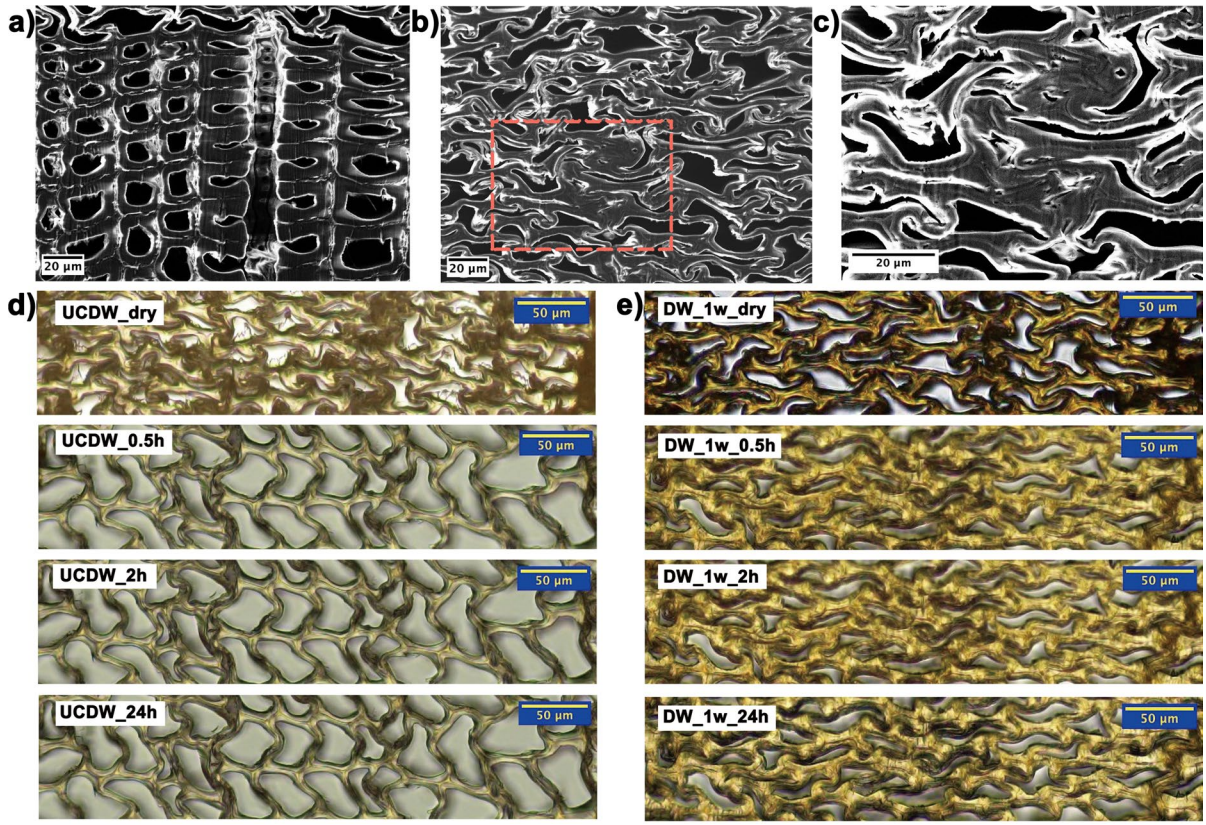

Fig. 4 SEM images (**a**-**c**) of DW_1w and Light micrographs (**d**, **e**) depicting the in-situ SR behavior of densified samples in water at different exposure times: **a** SEM image illustrates the latewood morphology in DW_1w; **b** and **c** the earlywood morphology in DW_1w and the magnified detail of the selected section (red dashed line); **d** and **e** the light micrographs demonstrate the respective in-situ morphology changes in UCDW and DW_1w

Molecular features and thermal properties of wood samples

The molecular features of the wood samples were assessed using ATR_FTIR as depicted in Fig. 5a-b. A notable peak at 1027 cm^{-1} accompanied by smaller shoulders at 1051 cm^{-1}, 1103 cm^{-1}, and 1155 cm^{-1} were observed in all samples. These absorbance bands correspond to the characteristic C–O–C stretching in the pyranose ring, indicative of cellulose and other carbohydrates (Çelik and Can 2023; Lan et al. 2011). Bands around 1232 cm^{-1} and 1261 cm^{-1} are assigned to the lignin aromatic structure (C = O and C-O groups in lignin), while bands at 1422 cm^{-1}, 1508 cm^{-1}, and 1603 cm^{-1} are attributed to aromatic skeletal vibrations (Lehto et al. 2018).

Evidently, the aforementioned peaks exhibit enhanced clarity and sharpness in the DW_1w spectrum when compared to the spectrum of UC. This intensified spectral resolution is likely attributed to the partial degradation of hemicellulose, a small amount of lignin, and volatile components during the densification and subsequent washing process (Hill 2006; Lehto et al. 2018). The degradation of hemicellulose and extractives can contribute to an increase in the relative portion of remaining lignin and cellulose in the DW_1w, which may lead to an augmentation in the absorbances associated with lignin and cellulose. Especially, this degradation is further corroborated by the observed reduction in absorbance at 1740 cm^{-1} in both DW_1 and DW_1w (Fig. 5b, encompassing the range from 1800 to 600 cm^{-1}), addressing the cleavage of acetyl groups from hemicellulose (Altgen et al. 2020). The observed results are further evidenced by the results (Table S2) of full chemical composition analysis in the SI.

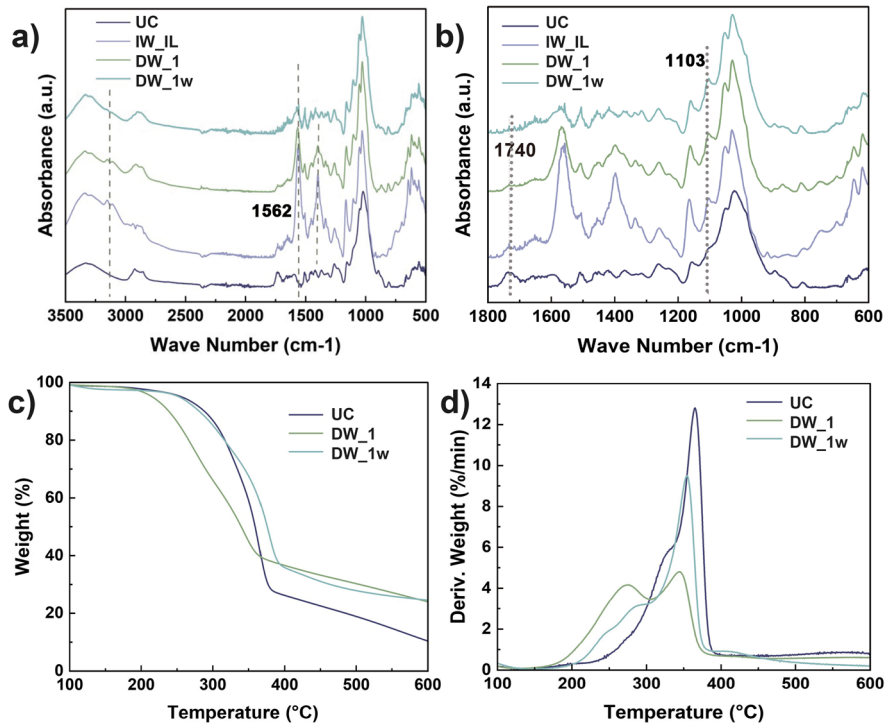

Fig. 5 Molecular features and thermal properties of wood samples: **a** and **b** are the FTIR absorbance spectrum of wood samples; **c** and **d** are thermal degradation behavior of the wood samples as a function of temperature

The presence of two distinct peaks in the IW_IL spectrum at 1378 cm^{-1} and 1562 cm^{-1} (dashed lines in Fig. 5a) can be attributed to the impregnation of wood specimens with the IL [emim][OAc]. These peaks are assigned to the symmetric and asymmetric O-C-O stretches of the acetic anion in pure [emim][OAc] (Tan et al. 2016; Zhang et al. 2015), as illustrated in Fig. S3b. Furthermore, the -OH absorbance bands in the range of 3100 cm^{-1} to 3300 cm^{-1}, are indicative of inter- and intra-molecular hydrogen bonding in cellulose, becoming more pronounced due to additional interactions with acetic anions (Tan et al. 2016). However, the intensity of these peaks, resulting from [emim][OAc], is slightly diminished in the spectrum of DW_1. This reduction could be caused by the interaction of the IL with the wood cell wall, which softens and plasticizes during the densification process. It is obvious that the signals indicating the presence of IL in DW_1w almost disappear because of washing with water, as shown in Fig. 5a-b. This suggests that the IL was leached out during the washing process. When comparing with the absorbance spectrum of UC, it can be concluded that the chemical structure (polymer constituents) of DW_1w remains unaltered, and no derivatization reactions occur when wood is subjected to the IL-densification process. This result can be further substantiated by examining the X-ray diffraction patterns of UC and DW_1w (Figure S2), where DW_1w demonstrated a similar diffraction pattern to that of UC but with increased intensity and slightly shifted peaks. This observation can be attributed to the cellulose repolymerization, enhanced crystallinity (partial degradation of hemicellulose and disordered cellulose) and enlarged crystal size (Table S3). IL impregnation shows substantial potential as a pretreatment for wood densification because it preserves the polymer constituents of wood while eliminating SR, as discussed above.

Thermogravimetric analysis (TGA) was conducted to assess the thermostability of IL treated DW. The TGA weight loss curves of the wood samples, accompanied by the derivative mass thermal degradation percentage per minute are shown in Fig. 5c and d, respectively. The outcome demonstrates that IL-treated DW (DW_1 and DW_1w) exhibits an enhanced thermostability in comparison to the UC in terms of the decomposition rate. Notably, UC experiences a substantial weight loss of approximately 70% within the temperature range of 245 to 400 °C,

with a residual weight of 10% at 600 °C (Fig. 5c). In contrast, both DW_1 and DW_1w exhibit a weight loss of 60% at 400 °C and retain 25% of their mass at 600 °C. Moreover, the rate of thermal degradation for DW_1 and DW_1w is slower than that of UC as the temperature increases (Fig. 5d).

However, the onset of thermal degradation for DW_1, as indicated by the derivative weight loss plot (Fig. 5d), occurs at approximately 202 °C (Table 2), with its first degradation peak appearing at 275 °C (Table 2). These values are lower than those observed for UC (Table 2). This deviation can be attributed to the decomposition of IL [emim][OAc], which is consistent with values reported in the literature, implying an onset degradation temperature of [emim][OAc] is between 200 and 221 °C, with a peak decomposition temperature around 250 °C (Cao and Mu 2014; Williams et al. 2018). While for UC, the T_{onset} exhibited at 245 °C is attributed to hemicellulose decomposition (Werner et al. 2014). The second degradation peak of DW_1 at 345 °C (Table 2) corresponds to the thermal degradation of crystalline cellulose (Liu et al. 2022). This degradation occurs at a significantly slower rate in the treated samples as compared to UC. This signifies the suppression of wood thermal degradation due to the IL treatment (Khakalo et al. 2020). Especially, when subjected to washing with water, DW_1w exhibits a delayed onset degradation temperature compared to non-washed DW_1 (Table 2). For DW_1w, the initial degradation peak at 248 °C could be assigned to the decomposition of hemicellulose, while the subsequent second (290 °C) and third (355 °C) peaks are associated with the partial degradation of cellulose molecules, which had been subjected to depolymerization and regeneration by [emim][OAc], as well as the decomposition of crystalline cellulose in DW_1w (Tan et al. 2019). This observation underlines the heightened thermal stability achieved through IL-based modification in combination with wood densification.

Table 2 Thermal degradation temperature of wood specimens

Sample	T_{onset} (°C)	T_{peak} (°C)
UC	245	330/365
DW_1	202	275/345
DW_1w	245	248/290/355

Furthermore, the water-washing process (involving ionic exchange and re-polymerization) of DW_1 did not negatively affect the thermostability and mechanical strength of DW_1w; on the contrary, it improved the thermostability compared to the unwashed specimen. Particularly noteworthy is the leached-out [emim][OAc], which is recyclable and recoverable for subsequent reuse. Additionally, the chemical structure analysis of DW_1w revealed similarities with that of UC (Fig. 5a), which indicates no chemical residue (IL) remaining in the wood specimens. This outcome unequivocally affirms the potential for recycling and cascading DW_1w products after their service life. Consequently, our proposed method achieves a recyclable densified wood with negligible SR, accomplished through a synergistic combination of IL pretreatment and water-washing in the post-treatment phase. Notably, this method addresses the inherent non-recyclability associated with conventionally produced DW using chemical techniques in the wood densification process.

Conclusions

The impregnation of wood with IL combined with densification resulted in negligible SR when exposed to liquid water. This finding is attributed to the plasticization of crystalline cellulose by IL [emim][OAc] within the cell wall during the densification process at 150 °C. Even though the densified wood experiences partial degradation of wood components like hemicellulose, amorphous cellulose, and a small amount of lignin, it still exhibits enhanced flexural strength and improved thermal stability compared to un-densified wood. Specifically, DW_1w achieved a 100% higher stiffness with a slower degradation rate at high temperatures. Therefore, within the frame of the research carried out in this work, wood densification and washing following IL impregnation demonstrates great potential for wood modification. This expands the scope of potential end-uses for low-density and undervalued wood materials, extending to applications exposed to humid conditions. Furthermore, the employed IL [emim][OAc] can be recovered and reused successfully, and the utilization of [emim][OAc] presents significant potential advantages in terms of promoting sustainable approaches in wood modification processes.

Subsequently, our forthcoming studies will focus on determining the purity and recovery rate of the recycled [emim][OAc], aiming to quantify the alternations in wood chemical compositions induced by [emim][OAc] and assess its impact on the material flexural strength. These investigations will provide further insights into the efficiency and environmental implications of the proposed wood modification process, contributing to the ongoing efforts in advancing sustainable practices within the field.

Author contributions S.Z. conceived the initial manuscript text, designed the research concept, conducted sample preparation, and analyzed experimental data. H.M. contributed to sample preparation, assisted in mechanical testing, and participated in manuscript revision. S.C. provided instructions for mechanical testing and revised the manuscript. T.L. reviewed the manuscript. L.R. supervised the research concept and manuscript revision. All authors participated in the manuscript review.

Funding Open Access funding provided by Aalto University. The authors declare that no funds, grants, or other support were received during the preparation of this manuscript.

Data availability No datasets were generated or analysed during the current study.

Declarations

Human and/or animals rights Not applicable.

Consent for publication Not applicable.

Competing interests The authors declare no competing interests.

References

Abushammala H, Mao J (2020) A review on the partial and complete dissolution and fractionation of wood and lignocelluloses using imidazolium ionic liquids. Polymers (Basel) 12:195. https://doi.org/10.3390/polym12010195

Abu-Eishah SI (2015) Utilization of ionic liquids in wood and wood-related applications — a review. In: ionic liquids - current state of the art. InTech

Altgen M, Awais M, Altgen D et al (2020) Micro-tensile behavior of Scots pine sapwood after heat treatments in superheated steam or pressurized hot water. J Mater Sci 55:12621–12635. https://doi.org/10.1007/s10853-020-04943-6

Cabral JP, Kafle B, Subhani M et al (2022) Densification of timber: a review on the process, material properties, and application. J Wood Sci 68. https://doi.org/10.1186/s10086-022-02028-3

Candelier K, Thevenon M-F, Petrissans A et al (2016) Control of wood thermal treatment and its effects on decay resistance: a review. Ann For Sci 73:571–583. https://doi.org/10.1007/s13595-016-0541-x

Cao Y, Mu T (2014) Comprehensive investigation on the thermal stability of 66 ionic liquids by thermogravimetric analysis. Ind Eng Chem Res 53:8651–8664. https://doi.org/10.1021/ie5009597

Çelïk AE, Can A (2023) Surface characterization of wood treated with acidic deep eutectic solvents. Eur J Wood Wood Prod 81:143–157. https://doi.org/10.1007/s00107-022-01843-1

Chen C, Kuang Y, Zhu S et al (2020) Structure–property–function relationships of natural and engineered wood. Nat Rev Mater 5:642–666. https://doi.org/10.1038/s41578-020-0195-z

Croitoru C, Roata IC (2020) Ionic liquids as antifungal agents for wood preservation. Molecules 25:4289. https://doi.org/10.3390/molecules25184289

Dong X, Gan W, Shang Y et al (2022) Low-value wood for sustainable high-performance structural materials. Nat Sustain 5:628–635. https://doi.org/10.1038/s41893-022-00887-8

Halder P, Kundu S, Patel S et al (2020) Investigation of reaction mechanism and the effects of process parameters on ionic liquid–based delignification of sugarcane straw. Bioenergy Res 13:1144–1158. https://doi.org/10.1007/s12155-020-10134-7

Halder P, Kundu S, Patel S et al (2019) A comparison of ionic liquids and organic solvents on the separation of cellulose-rich material from river Red Gum. Bioenergy Res 12:275–291. https://doi.org/10.1007/s12155-019-09967-8

Hill CAS (2006) Wood modification: chemical, thermal and other processes. Wiley-Blackwell, Wiley-Blackwell

Khakalo A, Tanaka A, Korpela A et al (2019) All-wood composite material by partial fiber surface dissolution with an ionic liquid. ACS Sustain Chem Eng 7:3195–3202. https://doi.org/10.1021/acssuschemeng.8b05059

Khakalo A, Tanaka A, Korpela A, Orelma H (2020) Delignification and ionic liquid treatment of wood toward multifunctional high-performance structural materials. ACS Appl Mater Interfaces 12:23532–23542. https://doi.org/10.1021/acsami.0c02221

Lan W, Liu C-F, Sun R-C (2011) Fractionation of bagasse into cellulose, hemicelluloses, and lignin with ionic liquid treatment followed by alkaline extraction. J Agric Food Chem 59:8691–8701. https://doi.org/10.1021/jf201508g

Lehto J, Louhelainen J, Kłosińska T et al (2018) Characterization of alkali-extracted wood by FTIR-ATR spectroscopy. Biomass Convers Biorefin 8:847–855. https://doi.org/10.1007/s13399-018-0327-5

Ling Z, Chen S, Zhang X et al (2017) Unraveling variations of crystalline cellulose induced by ionic liquid and their effects on enzymatic hydrolysis. Sci Rep 7. https://doi.org/10.1038/s41598-017-09885-9

Liu B, Li W, Xu Y et al (2022) Mechanism of cellulose regeneration from its ionic liquid solution as revealed by infrared spectroscopy. Polymer (Guildf) 257:125280. https://doi.org/10.1016/j.polymer.2022.125280

Liu C, Luan P, Li Q et al (2021) Biopolymeric materials: Biopolymers derived from trees as sustainable multifunctional materials: a review. Adv Mater 33. https://doi.org/10.1002/adma.202170220

Luan Y, Fang C-H, Ma Y-F, Fei B-H (2022) Wood mechanical densification: a review on processing. Mater Manuf Process 37:359–371. https://doi.org/10.1080/10426914.2021.2016816

Miyafuji H, Fujiwara Y (2013) Fire resistance of wood treated with various ionic liquids (ILs). Holzforschung 67:787–793. https://doi.org/10.1515/hf-2012-0166

Miyafuji H, Minamoto K (2022) Fire and termite resistance of wood treated with PF6-based ionic liquids. Sci Rep 12. https://doi.org/10.1038/s41598-022-18792-7

Miyafuji H, Miyata K, Saka S et al (2009) Reaction behavior of wood in an ionic liquid, 1-ethyl-3-methyli-midazolium-chloride. J Wood Sci 55:215–219. https://doi.org/10.1007/s10086-009-1020-x

Nakaya N, Hosoya T, Miyafuji H (2018) Ionic liquids as formaldehyde-free wood adhesives. J Wood Sci 64:794–801. https://doi.org/10.1007/s10086-018-1769-x

Neyses B, Karlsson O, Sandberg D (2020) The effect of ionic liquid and superbase pre-treatment on the spring-back, set-recovery and Brinell hardness of surface-densified Scots pine. Holzforschung 74:303–312. https://doi.org/10.1515/hf-2019-0158

Neyses B, Peeters K, Buck D et al (2021) *In-situ* penetration of ionic liquids during surface densification of Scots pine. Holzforschung 75:555–562. https://doi.org/10.1515/hf-2020-0146

Orelma H, Tanaka A, Vuoriluoto M et al (2021) Manufacture of all-wood sawdust-based particle board using ionic liquid-facilitated fusion process. Wood Sci Technol 55:331–349. https://doi.org/10.1007/s00226-021-01265-x

Qasim U, Rafiq S, Jamil F et al (2021) Processing of lignocellulose in ionic liquids: a cleaner and sustainable approach. J Clean Prod 323:129189. https://doi.org/10.1016/j.jclepro.2021.129189

Rautkari L, Properzi M, Pichelin F, Hughes M (2010) Properties and set-recovery of surface densified Norway spruce and European beech. Wood Sci Technol 44:679–691. https://doi.org/10.1007/s00226-009-0291-0

Rissman J, Bataille C, Masanet E et al (2020) Technologies and policies to decarbonize global industry: review and assessment of mitigation drivers through 2070. Appl Energy 266:114848. https://doi.org/10.1016/j.apenergy.2020.114848

SFS-EN 310:en (2001) In: Sfs.fi. https://sales.sfs.fi/fi/index/tuotteet/SFS/CEN/ID2/3/9704.html.stx. Accessed 6 Mar 2024

Song J, Chen C, Zhu S et al (2018) Processing bulk natural wood into a high-performance structural material. Nature 554:224–228. https://doi.org/10.1038/nature25476

Sun N, Rahman M, Qin Y et al (2009) Complete dissolution and partial delignification of wood in the ionic liquid 1-ethyl-3-methylimidazolium acetate. Green Chem 11:646. https://doi.org/10.1039/b822702k

Tan X, Chen L, Li X, Xie F (2019) Effect of anti-solvents on the characteristics of regenerated cellulose from 1-ethyl-3-methylimidazolium acetate ionic liquid. Int J Biol Macromol 124:314–320. https://doi.org/10.1016/j.ijbiomac.2018.11.138

Tan X, Li X, Chen L, Xie F (2016) Solubility of starch and microcrystalline cellulose in 1-ethyl-3-methylimidazolium acetate ionic liquid and solution rheological properties. Phys Chem Chem Phys 18:27584–27593. https://doi.org/10.1039/c6cp04426c

Werner K, Pommer L, Broström M (2014) Thermal decomposition of hemicelluloses. J Anal Appl Pyrolysis 110:130–137. https://doi.org/10.1016/j.jaap.2014.08.013

Williams ML, Holahan SP, McCorkill ME et al (2018) Thermal and spectral characterization and stability of mixtures of ionic liquids [EMIM]Ac and [BMIM]Ac with ethanol, methanol, and water at ambient conditions and at elevated temperatures and pressures. Thermochim Acta 669:126–139. https://doi.org/10.1016/j.tca.2018.09.013

Xu B-H, Liu K, Bouchaïr A (2020) Mechanical properties and set recovery of compressed poplar with glycerin pretreatment. Wood Res 65:293–302. https://doi.org/10.37763/wr.1336-4561/65.2.293302

Zhang B, Chen L, Xie F et al (2015) Understanding the structural disorganization of starch in water–ionic liquid solutions. Phys Chem Chem Phys 17:13860–13871. https://doi.org/10.1039/c5cp01176k

Zhang S, Reyes G, Khakalo A, Rojas OJ (2024) Hollow filaments from coaxial dry–jet wet spinning of a cellulose solution in an ionic liquid: Wet-strength and water interactions. Biomacromol 25:282–289. https://doi.org/10.1021/acs.biomac.3c00984